

## Selective reversible inhibition of human butyrylcholinesterase by aryl amide derivatives of phenothiazine

Sultan Darvesh,<sup>a,b,c,\*</sup> Robert S. McDonald,<sup>c</sup> Katherine V. Darvesh,<sup>c</sup> Diane Mataija,<sup>c</sup> Sarah Conrad,<sup>c</sup> Geraldine Gomez,<sup>c</sup> Ryan Walsh<sup>b</sup> and Earl Martin<sup>c</sup>

<sup>a</sup>Department of Medicine (Neurology), Dalhousie University, Halifax, NS, Canada

<sup>b</sup>Department of Anatomy and Neurobiology, Dalhousie University, Halifax, NS, Canada

<sup>c</sup>Department of Chemistry, Mount Saint Vincent University, Halifax, NS, Canada

Received 13 March 2007; revised 22 June 2007; accepted 29 June 2007

Available online 6 July 2007

**Abstract**—Evidence suggests that specific inhibition of butyrylcholinesterase may be an appropriate focus for the development of more effective drugs to treat dementias such as Alzheimer's disease. Butyrylcholinesterase is a co-regulator of cholinergic neurotransmission and its activity is increased in Alzheimer's disease, and is associated with all neuropathological lesions in this disease. Some selective butyrylcholinesterase inhibitors have already been reported to increase acetylcholine levels and to reduce the formation of abnormal amyloid found in Alzheimer's disease. Synthesized *N*-(10)-aryl and *N*-(10)-alkylaryl amides of phenothiazine are specific inhibitors of butyrylcholinesterase. In some cases, inhibition constants in the nanomolar range are achieved. Enzyme specificity and inhibitor potency of these molecules can be related to molecular volumes, steric and electronic factors. Computed log *P* values indicate high potential for these compounds to cross the blood–brain barrier. Use of such butyrylcholinesterase inhibitors could provide direct evidence for the importance of this enzyme in the normal nervous system and in Alzheimer's disease. © 2007 Elsevier Ltd. All rights reserved.

### 1. Introduction

In Alzheimer's disease (AD), there is a severe loss of cholinergic cells in the brain that leads to diminished levels of the neurotransmitter acetylcholine.<sup>1,2</sup> These changes are considered responsible for the salient cognitive and behavioral symptoms that occur in this disease.<sup>3,4</sup> Acetylcholinesterase (AChE, EC 3.1.1.7) and butyrylcholinesterase (BuChE, EC 3.1.1.8) are serine hydrolase enzymes that effect the breakdown of acetylcholine.<sup>5</sup> Therefore, inhibition of these enzymes has proven a successful approach to treat some of the symptoms of AD.<sup>6</sup> However, in AD, AChE levels in the brain are already decreased, while BuChE activity is elevated<sup>7–9</sup> suggesting that acetylcholine hydrolysis in AD may occur to a greater extent via BuChE catalysis.<sup>10</sup> In this regard, it has been reported that the specific inhibition of

BuChE is important in raising acetylcholine levels and improving cognition.<sup>11,12</sup> Cholinesterase inhibitors currently in use to treat AD inhibit both AChE and BuChE,<sup>13</sup> and with these drugs it is difficult to determine whether the positive effects observed are a result of inhibition of AChE, BuChE or both enzymes. For this reason, it is important to test selective, potent and well-tolerated inhibitors of each individual cholinesterase in order to determine which enzyme needs to be the focus for maximum effect in treating AD.<sup>14</sup>

The inhibition of cholinesterase activity requires that the inhibitor bind with the enzyme so that the substrate is partially or completely blocked from normal interaction with the catalytic site. In some instances, this substrate interference can be transient, as in the case of reversible inhibitors like donepezil<sup>15</sup> and galantamine.<sup>16</sup> On the other hand, the catalytic site can be compromised for longer periods by covalent bond formation at the active site serine, as is the case with the pseudo-irreversible inhibitors, physostigmine<sup>17</sup> and rivastigmine.<sup>18</sup> Differences between AChE and BuChE in the region of the active site can be exploited in developing inhibitors that are selective for one cholinesterase over the other.

**Keywords:** Cholinesterase; Alzheimer's disease; Molecular modeling; Partition coefficient.

\* Corresponding author at present address: Room 1308, Camp Hill Veterans' Memorial Building 1, 5955 Veterans' Memorial Lane, Halifax, NS, Canada B3H 2E1. Tel.: +1 902 473 2490; fax: +1 902 473 7133; e-mail: [sultan.darvesh@dal.ca](mailto:sultan.darvesh@dal.ca)

Both AChE and BuChE have a catalytic site that is near the bottom of a 20 Å deep gorge in the protein.<sup>19,20</sup> Distinct amino acid residues in the gorge of AChE and BuChE help explain the more selective binding of an inhibitor such as donepezil to AChE.<sup>21</sup> One stabilizing factor for the binding of this compound to AChE involves interaction of the indanone moiety of the inhibitor with W286 near the mouth of the gorge, a residue that is different (A277) in BuChE. This unique interaction of donepezil with AChE would be expected to contribute to the several hundred-fold greater potency of this inhibitor toward AChE than for BuChE.<sup>22</sup>

At the bottom of the active site cholinesterase gorge is a triad of residues responsible for catalyzing the hydrolysis of choline esters and aryl amides<sup>23</sup> and is comprised of serine, histidine, and glutamate.<sup>19,20</sup>

In AChE, the estimated volume of the active site gorge is relatively small (302 Å<sup>3</sup>), being lined with 14 bulky aromatic amino acid residues, while that of BuChE, with only 8 aryl residues, is considerably larger in volume (502 Å<sup>3</sup>).<sup>20,24</sup> This difference in gorge volume can play a role in determining the size of inhibitor molecules that can be accommodated by the active site of each enzyme, thus providing one means of inhibitor selectivity.<sup>24,25</sup>

Other unique features of the active site gorge regions of AChE and BuChE may also play a part in inhibitor selectivity. For example, phenothiazine and many of its derivatives are selective inhibitors of BuChE,<sup>26,27</sup> even when they have molecular volumes smaller than the AChE gorge.<sup>27</sup> In BuChE,  $\pi$ - $\pi$  interaction has been reported to take place between the phenothiazine tricyclic ring system and the aromatic residues F329 and Y332, near the top of the gorge.<sup>24</sup> In AChE, an additional aromatic residue, tyrosine (Y337), interferes with this binding process and, hence, the same  $\pi$ - $\pi$  interaction cannot occur to bind phenothiazine to this enzyme. In human BuChE the equivalent residue (A328) does not interfere with this binding. Replacement of this hindering tyrosine residue with alanine, through site-directed mutagenesis, greatly enhanced the inhibition of this AChE by the phenothiazine derivative ethopropazine.<sup>24</sup>

In general, *N*-(10)-alkyl amide derivatives of phenothiazine are inhibitors of BuChE, and only a few smaller molecules in this class are capable of inhibiting AChE.<sup>25</sup> The observation that larger phenothiazine molecules were more specific for BuChE prompted the present work in a search for more potent specific BuChE inhibitors.

Here we report the synthesis and inhibitor properties of a series of *N*-(10)-aryl and *N*-(10)-alkylaryl amide derivatives of phenothiazine that are reversible specific inhibitors of BuChE. These derivatives can be made to provide inhibition levels ( $K_i$  values) in the nanomolar range. Comparative effects of increasing molecular volume, altering ring substitution and ring substituent position in the aryl and alkylaryl derivatives, provide new insights into structural changes that influence the binding of phenothiazines to BuChE, affecting its catalytic

activity. Also examined are certain other structural parameters, as well as electronic considerations, that can affect BuChE inhibition. The significant hydrophobic nature of these aromatic phenothiazine amides, represented by calculated partition coefficients (log *P* values; octanol/water), indicates potential for crossing the blood–brain barrier for direct inhibition of brain BuChE.

## 2. Results and discussion

A total of 25 derivatives of phenothiazine were synthesized (Table 1 and Fig. 1). All the derivatives were *N*-(10)-amides with variously substituted aryl and alkylaryl side groups. These derivatives were examined for their ability to inhibit BuChE and AChE. None of the compounds tested showed AChE inhibition, up to their solubility limit ( $3.33 \times 10^{-5}$ – $1.67 \times 10^{-4}$  M), under assay conditions.

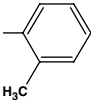
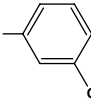
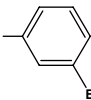
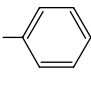
### 2.1. Synthetic chemistry

The *N*-substituted aryl and alkylaryl phenothiazine amides were prepared by refluxing, in dichloromethane, phenothiazine and excess acid chloride (Fig. 1), and an equivalent amount of triethylamine to neutralize HCl released during reaction. Purification of the derivatives was performed by sequential chemically active extraction, silica gel column chromatography and crystallization. All purified compounds were homogeneous by thin layer chromatographic analysis, and <sup>1</sup>H NMR revealed all of them to be more than 98% pure. All compounds were fully characterized by IR, <sup>1</sup>H and <sup>13</sup>C NMR spectroscopy, as well as low- and high-resolution (accurate mass) mass spectrometry. Physical data were consistent with the structure (Table 1) of each molecule synthesized.

### 2.2. Enzyme kinetic studies

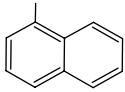
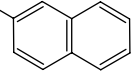
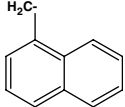
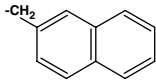
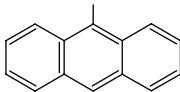
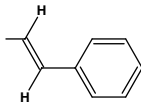
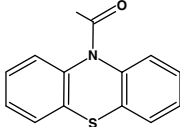
Each phenothiazine derivative was evaluated for its ability to inhibit purified human plasma BuChE and purified recombinant human AChE, using Ellman's spectrophotometric method.<sup>28</sup> Initially, each derivative was examined for cholinesterase inhibition at the highest inhibitor concentration, depending on solubility limits (up to 0.167 mM in 50% aqueous acetonitrile), and then through serial (1:10) dilutions in the same solvent to obtain an inhibition–concentration profile that indicated a range of inhibitor concentrations suitable for kinetic studies. The final concentration of acetonitrile (1.67% v/v), in the Ellman assays, was found to have no measurable effect on the activity of BuChE. Lineweaver–Burk plots were then generated for each compound in the absence of inhibitor and at two concentrations of inhibitor. A replot of slopes of these lines against inhibitor concentration gave the inhibition constant ( $K_i$  value, Table 1 and Fig. 2) as the intercept on the *x*-axis. The inhibition constant ( $K_i$ ) represents the equilibrium constant for the dissociation of the enzyme–inhibitor complex (EI) into enzyme (E) and inhibitor (I) {EI → E + I, where  $K_i = [E][I]/[EI]$ }. A small  $K_i$  value indicates a

**Table 1.** Inhibition constants, molecular volumes, and log *P* values of the synthesized phenothiazine amide derivatives

Compound	Derivative	R=	BuChE $K_i$ ( $\mu\text{M}$ ) <sup>a</sup>	Volume ( $\text{\AA}^3$ )	log <i>P</i> value
1	Benzoyl		$5.8 \pm 0.6$	$314 \pm 13$	4.57
2	2-Methylbenzoyl		$3.1 \pm 1.3$	$342 \pm 7$	4.71
3	3-Methylbenzoyl		$1.9 \pm 0.2$	$330 \pm 16$	4.70
4	3-Bromobenzoyl		$0.60 \pm 0.06$	$343 \pm 11$	4.96
5	4-Methylbenzoyl		$2.5 \pm 0.3$	$321 \pm 17$	4.70
6	4-Bromobenzoyl		$1.3 \pm 0.1$	$338 \pm 12$	4.93
7	4-Methoxybenzoyl		$1.5 \pm 0.5$	$350 \pm 16$	4.43
8	4-Acetoxybenzoyl		$23 \pm 9$	$374 \pm 11$	4.56
9	4-Nitrobenzoyl		$0.82 \pm 0.09$	$329 \pm 6$	4.43
10	4- <i>tert</i> -Butylbenzoyl		None <sup>b</sup>	$392 \pm 20$	5.83
11	4-Biphenylcarbonyl		None <sup>b</sup>	$389 \pm 22$	5.75
12	Phenylacetyl		$0.61 \pm 0.10$	$340 \pm 18$	4.66
13	2-Phenylpropanoyl		$0.56 \pm 0.12$	$376 \pm 22$	5.10
14	3-Phenylpropanoyl		$6.2 \pm 0.8$	$353 \pm 18$	4.84
15	2-Phenylbutanoyl		$0.40 \pm 0.03$	$383 \pm 16$	5.38
16	3-Phenylbutanoyl		$1.7 \pm 0.2$	$387 \pm 14$	5.25
17	4-Phenylbutanoyl		$0.22 \pm 0.05$	$392 \pm 26$	5.14
18	4-Biphenylacetyl		$1.7 \pm 0.4$	$430 \pm 19$	5.86

(continued on next page)

Table 1 (continued)

Compound	Derivative	R=	BuChE $K_i$ ( $\mu\text{M}$ ) <sup>a</sup>	Volume ( $\text{\AA}^3$ )	log $P$ value
19	1-Naphthoyl		$0.088 \pm 0.007$	$383 \pm 12$	5.47
20	2-Naphthoyl		$0.47 \pm 0.03$	$379 \pm 27$	5.47
21	1-Naphthylacetyl		$0.090 \pm 0.010$	$381 \pm 9$	5.57
22	2-Naphthylacetyl		$0.028 \pm 0.012$	$365 \pm 14$	5.59
23	9-Anthrylcarbonyl		$0.0035 \pm 0.0006$	$410 \pm 16$	6.31
24	<i>trans</i> -3-Phenylpropenoyl		$2.7 \pm 0.4$	$346 \pm 17$	5.59
25	Oxalyl(di)phenothiazine		$0.22 \pm 0.05$	$446 \pm 21$	4.74

<sup>a</sup> For comparison, the known compound galantamine inhibits BuChE ( $K_i = 2.09 \mu\text{M}$ ) as well as AChE ( $K_i = 1.08 \mu\text{M}$ ).<sup>13</sup> None of the phenothiazine amides inhibited AChE up to their solubility limits ( $3.33 \times 10^{-5}$ – $1.67 \times 10^{-4}$  M).

<sup>b</sup> None refers to no detectable inhibitory activity up to the solubility limit of these compounds ( $3.33 \times 10^{-5}$ – $1.67 \times 10^{-4}$  M) in the assay.

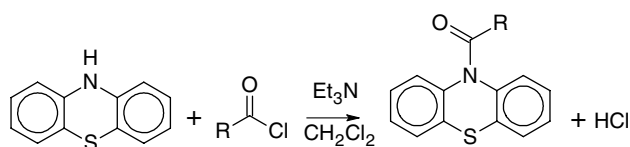


Figure 1. Scheme for the synthesis of *N*-(10)-substituted phenothiazine amide derivatives. The R groups are shown in Table 1.

higher inhibitor potency. The inhibitor potency ( $K_i$ ) was found to vary greatly between compounds, and the factors contributing to this were explored by considering molecular parameters related to the structure of each compound and to that of the enzyme.

### 2.3. Molecular computational studies

Computational methods were used to determine molecular characteristics that governed specificity and potency for cholinesterase inhibition. These parameters included total molecular volumes, as well as the measurement of length and width of certain substituent groups. The log  $P$  values were calculated to predict the ability of the compounds to cross the blood–brain barrier.

The molecular parameters that were examined were derived from molecular mechanics calculations of the

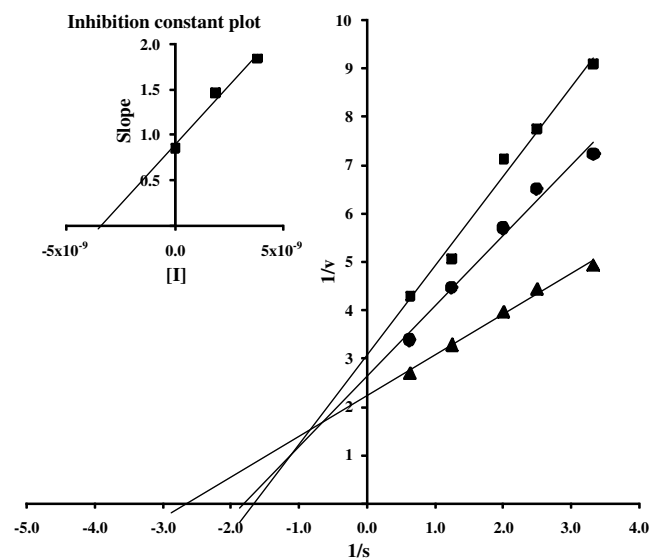


Figure 2. Lineweaver–Burk plot of butyrylcholinesterase (0.05 U) with substrate butyrylthiocholine, in the absence or presence of the inhibitor 9-anthrylcarbonyl phenothiazine amide (23). (▲) no inhibitor; (●)  $1.7 \times 10^{-9}$  M; (■)  $3.3 \times 10^{-9}$  M (23). Replot of the slopes of the lines versus  $[I]$  gave  $K_i$  as the  $x$ -intercept (inset).

minimum energy and preferred conformation for each derivative. Single-point calculations of molecular

volume for each compound were carried out at the HF/STO-3G level of theory,<sup>29</sup> at the geometry obtained using the MMFF94 force field method (PC Spartan Pro, Wavefunction, Inc., 18401 Von Karman, Suite 370, Irvine, California, 92612). These molecular volumes, based on an average of five calculations, are summarized in Table 1.

$\log P$  value has been used to estimate the facility with which a compound will cross the blood–brain barrier by diffusion. Experimentally, this is done by partitioning the molecule between water and the hydrophobic solvent *n*-octanol, and determining the  $P$  value as the ratio of the concentration of the compound in *n*-octanol and that in water. Often the solubility of a molecule in water is insufficient for the spectrophotometric analysis required in the experimental determination of  $\log P$  values. In such cases, values can be obtained indirectly via methods such as the ALOGPS v 2.0 system used herein.<sup>30</sup> This method compares the structure of the molecule with a large database of known molecular partition coefficients. The larger the value of  $\log P$ , the greater the hydrophobic nature of the molecule and, hence, the greater the facility with which it can cross the blood–brain barrier. All of the phenothiazine derivatives examined had calculated  $\log P$  values greater than 4.4 (Table 1). These partition coefficient values are all comparable to those calculated earlier for other phenothiazine derivatives.<sup>27</sup> In addition, although factors other than hydrophobicity may be involved in crossing the blood–brain barrier, the  $\log P$  values in Table 1 can be compared to those calculated here by the same method, for donepezil (4.14), galantamine (1.39), rivastigmine (2.59), tetrahydroaminoacridine (3.13), and ethopropazine (5.47), all compounds successful in treatment of diseases of the central nervous system.<sup>6,31</sup>

#### 2.4. Structure–activity relationships

A number of lines of evidence have indicated that phenothiazine derivatives bind to BuChE by interacting with two aromatic amino acid residues, F329 and Y332, through  $\pi$ – $\pi$  interaction, with the two aromatic rings of the phenothiazine tricycle.<sup>24,25</sup> With this common binding event, the differences in inhibitor potency ( $K_i$  values) were considered in terms of a number of molecular parameters.

**2.4.1. Effect of molecular volume.** The calculated total molecular volumes of the phenothiazine amides (Table 1) ranged from 314 Å<sup>3</sup> for the benzoyl derivative (1) to 446 Å<sup>3</sup> for the phenothiazine dimer of oxalic acid (25). The volumes of all the derivatives were larger than the estimated active site gorge volume of AChE (302 Å<sup>3</sup>) and smaller than that estimated for BuChE (502 Å<sup>3</sup>).<sup>24</sup> This provides one plausible explanation for the lack of AChE inhibition observed for all derivatives examined herein, since the smallest derivative (1) has a molecular volume that is greater than that of the active site gorge of this enzyme.

The extent of BuChE inhibition by phenothiazine amides was often found to be related to the total

molecular volume of the inhibitor (Table 1). For comparable derivatives this relationship was often linear, as exemplified by benzoyl (1), 1-naphthoyl (19), and 9-anthrylcarbonyl (23) amide derivatives. In this grouping, the largest derivative (23) was over 1000-fold more potent as a BuChE inhibitor than the smallest (1), while that of the intermediate sized molecule, 19, was roughly 100-fold more potent than compound 1 (Table 1). The direct relationship between inhibitor potency and molecular volume was also observed with other comparable series, such as benzoyl (1), 4-methylbenzoyl (5), and 4-methoxybenzoyl (7), and between the phenylacetyl (12), 2-phenylpropanoyl (13), and 2-phenylbutanoyl (15) derivatives (Table 1). However, the derivative with the largest volume, the phenothiazine dimer of oxalic acid (25) (volume = 446 Å<sup>3</sup>), is 60-fold less inhibitory than the 9-anthrylcarbonyl derivative (23), which has a smaller total volume (410 Å<sup>3</sup>) (Table 1). Thus, total molecular volume alone cannot account for the variety of inhibitor potencies for these phenothiazine derivatives. Thus, even the simplest apparent linear relationship between molecular volume and inhibitor potency may be more complex on closer examination and be attributable to multiple factors.

Earlier studies of the specific inhibition of BuChE by the phenothiazine derivative ethopropazine, using molecular dynamics calculations and site-directed mutagenesis,<sup>24</sup> indicated the importance of two aromatic amino acid residues in the enzyme, F329 and Y332. These residues permit  $\pi$ – $\pi$  interaction with the tricyclic system of phenothiazine. Thus, the phenothiazine moiety of compounds such as 1, 19, and 23 binds in a comparable way to the aryl side groups of F329 and Y332, but the broadest, tricyclic 9-anthryl group of 23 is superior in its

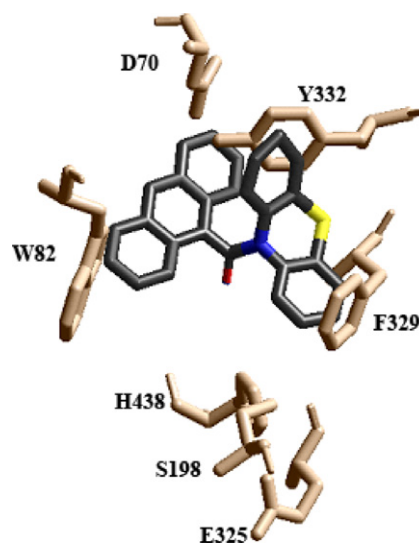


**Figure 3.** Simulated interaction of 9-anthrylcarbonyl phenothiazine amide (23) showing binding of the phenothiazine moiety to F329 and Y332 in the active site gorge of human butyrylcholinesterase. This figure was generated using the crystal structure of butyrylcholinesterase,<sup>20</sup> obtained from the protein databank,<sup>40</sup> and using PyMol<sup>41</sup> and HyperChem program<sup>42</sup> and by manually placing 23 in the active site gorge.

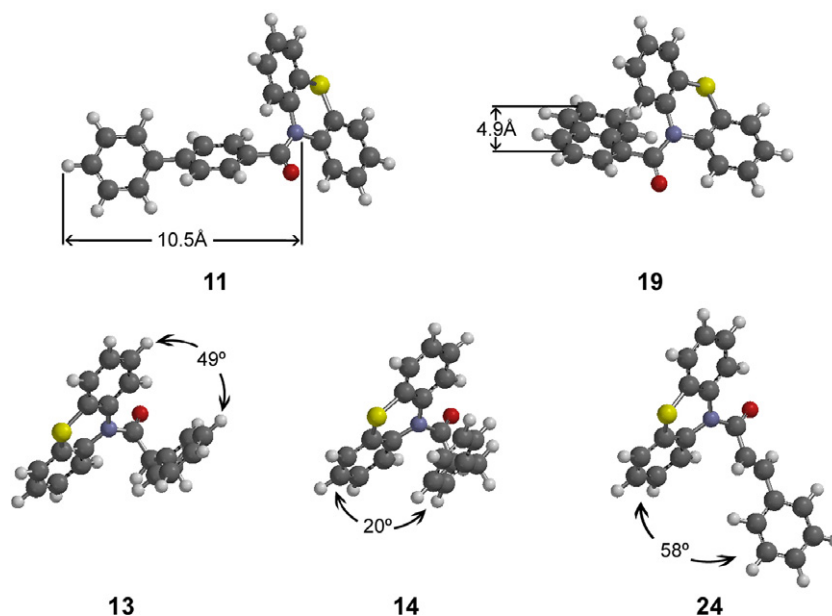


**Figure 4.** Conformation effects influencing butyrylcholinesterase inhibition. In compound **11**, the extended nature of the substituent, reflected in the distance from the N of the phenothiazine moiety to the most distal end of the side group, interferes with butyrylcholinesterase inhibition. In **19**, the comparable distance is only 6.2 Å. Preferred conformation models of comparable derivatives **13**, **14** and **24** indicate the much closer proximity of the planes of the aromatic rings in **14** facilitating intramolecular  $\pi$ - $\pi$  interaction and leading to decreased enzyme inhibition.

ability to block substrate access to the catalytic triad (Fig. 3) than is the bicyclic naphthyl group of **19** which, in turn, is more effective than the smaller phenyl moiety of **1** (Table 1). This ability to block substrate can be explained by the difference in the width of the substituent planar aryl moiety of these compounds, calculated to be 2.4, 4.9, and 7.3 Å, for the phenyl, naphthyl and anthryl groups, respectively (see Fig. 4 for an illustration of width determination).

**2.4.2. Effect on inhibition of substituents on the aryl moiety.** Substitution of the aryl amide derivatives of phenothiazine showed measurable effects on BuChE inhibition. Introduction of small substituents such as methyl showed very limited effects with respect to the position (*ortho*-, *meta*- or *para*-) on the benzene ring, although the *meta* position appeared to be slightly favored (Table 1). Overall, most substituted aryl derivatives were somewhat more potent than the parent compound (**1**). However, three of the larger *para*-substituted benzoyl derivatives showed a dramatic reduction in the ability to inhibit BuChE, despite favorable total molecular volumes. For example, the 4-acetoxybenzoyl derivative (**8**) (volume = 374 Å<sup>3</sup>) had a considerably weakened ability to inhibit BuChE ( $K_i$  = 23 μM), compared to the unsubstituted benzoyl derivative (**1**) ( $K_i$  = 5.8 μM). In fact, the larger derivatives 4-*tert*-butylbenzoyl (**10**) (volume = 392 Å<sup>3</sup>) and 4-biphenylcarbonyl (**11**) (volume = 389 Å<sup>3</sup>) did not inhibit BuChE at all. This lack of ability to inhibit BuChE is not simply an excessive volume effect since the larger 9-anthrylcarbonyl derivative (**23**) (volume = 410 Å<sup>3</sup>) was the most powerful BuChE inhibitor (Table 1), and all of these compounds (**10**, **11**, and **23**) are smaller than the estimated BuChE active site gorge volume (502 Å<sup>3</sup>).<sup>24</sup> These observations are more consistent with steric interference

related to the requisite intermolecular binding of the phenothiazine ring system to the active site residues F329 and Y332 in the gorge (Fig. 3). This steric interference was considered to be due to the extended substituent length, rather than the total volume, of these compounds. The rigid nature of these molecules, arising from the conjugation of the benzoyl moiety with the phenothiazine amide bond, combined with the excessive length of the entire substituent in **10** and **11**, prevents the correct alignment of the phenothiazine ring system in the active site gorge for proper binding to F329 and Y332. In preferred conformations, the conjugated substituent aryl moiety in **11** is almost at 90° to the phenothiazine tricycle. The distance from the phenothiazine nitrogen to the most distal hydrogen of the benzoyl (**1**), 1-naphthoyl (**19**), and 9-anthrylcarbonyl (**23**) derivatives, that is, the length of each substituent, is roughly 6.2 Å. On the other hand, the same distance for the 4-*tert*-butylbenzoyl derivative (**10**) is 8.6 Å and that for the biphenylcarbonyl (**11**) is 10.5 Å (see Fig. 4 for an illustration of length determination). Thus, the limited width of the BuChE active site gorge and the excessive lengths of the rigid 4-*tert*-butylbenzoyl (**10**) and 4-biphenylcarbonyl (**11**) derivatives must interfere with the alignment of the phenothiazine tricycle with F329 and Y332 for  $\pi$ - $\pi$  interaction. Support for this notion also comes from the observation that, when this conformational rigidity is relieved by the introduction of a methylene group between the carbonyl and the phenyl group, as in the 4-biphenylacetyl derivative (**18**), BuChE inhibition, absent in **11**, is restored in **18** (Table 1). Furthermore, the fact that this compound (**18**) has a volume of 430 Å<sup>3</sup>, larger than that for the 4-biphenylcarbonyl derivative (**11**), lends support to the notion that lack of BuChE inhibition with **10** and **11** is related to the rigidity and length of these compounds, rather than to

excessive total molecular volume effects. Furthermore, confirmation that shape (steric effects), rather than volume, can be a factor in determining inhibitor potency, comes from comparing another series of comparable derivatives. The biphenylacetyl (**18**), 1-naphthylacetyl (**21**) and 2-naphthylacetyl (**22**) are all comparable in molecular weight, but the largest, in terms of molecular volume (**18**) (Table 1), is the poorest BuChE inhibitor, while the molecule with the smallest volume (**22**) is almost 20 times more effective than **21** and 60 times better than **18**. In addition, comparing the above compounds with the phenylacetyl derivative (**12**) indicates that the naphthylacetyl derivatives (**21** and **22**) show the expected increase in inhibitor potency over compound **12**, based on volume considerations. However, the biphenylacetyl derivative (**18**) shows no correlation with **12**, based on volume alone. This is a further indication that the length of the biphenylacetyl derivative (**18**), although improved over the biphenylcarbonyl (**11**), is still interfering with the phenothiazine moiety binding to BuChE.

#### 2.4.3. Effect of substituent aromatic nucleus orientation.

The 1- and 2-naphthoyl derivatives (**19** and **20**, respectively), along with the 1- and 2-naphthylacetyl compounds (**21** and **22**, respectively), also provide some insight into structure–activity relationships. Compound **19** is a fivefold more potent inhibitor than the isomeric **20**. Presumably this is an orientation effect since both of these molecules are conformationally rigid. Introducing a methylene group between the 2-naphthyl ring system and the carbonyl (**20** → **22**) had a very large effect, increasing the BuChE-inhibiting potency by 16-fold. On the other hand, the presence of the methylene group between the 1-naphthyl ring system and the carbonyl (**19** → **21**) produced no improvement in inhibition, indicating that the rigid 1-naphthoyl derivative (**19**) was already in proper orientation for optimal interference with substrate access to the catalytic site. Clearly, the precise orientation and conformation of the naphthyl ring system, when conjugated through the amide linkage, can have a profound effect on the potency of BuChE inhibition for these phenothiazine derivatives.

Another anomaly, again not related to volume, is demonstrated by the series of alkylaryl amides (**13**–**17**). In this grouping, having a phenyl group two carbons removed from the carbonyl resulted in a significant loss of inhibitor potency. Thus, the 3-phenylalkyl amides (**14** and **16**) are distinctly poorer inhibitors, by 4- to 8-fold, than the comparable 2- and 4-phenylalkyl amide isomers (**13**, **15**, and **17**) (Table 1). Since the volumes of the comparable derivatives in each set (**13/14** and **15/16/17**) are roughly the same, the difference in inhibitor potency cannot be attributed to this molecular parameter. However, determination of the most stable conformation of the 3-phenyl derivatives, such as **14**, revealed that, in their preferred conformation, these isomers permit the closest intramolecular interaction between the substituent phenyl group and the aromatic ring system of the phenothiazine, as indicated by a small angle between the aromatic ring planes in this derivative (Fig. 4). The intramolecular  $\pi$ – $\pi$  interactions present in the 3-phenylalkyl derivatives most likely diminish the

required intermolecular  $\pi$ – $\pi$  interaction between the phenothiazine tricycle and aromatic residues F329 and Y332 in the BuChE active site gorge. In the preferred conformation of 2-phenylpropanoyl (**13**), the substituent phenyl ring is further separated from the phenothiazine tricycle, leading to decreased intramolecular  $\pi$ – $\pi$  interaction and permitting the aromatic tricycle of the phenothiazine moiety to form better intermolecular  $\pi$ – $\pi$  interaction with the enzyme. A similar line of reasoning can account for the more powerful inhibition of BuChE by the *trans*-3-phenylpropenoyl derivative (**24**), compared to the analogous saturated compound **14**, since the conformationally rigid nature of the double bond in **24** (Fig. 4) would discourage the intramolecular  $\pi$ – $\pi$  interaction considered to be responsible for the lower BuChE inhibition potency exhibited by **14**.

### 3. Conclusions

The *N*-(10)-aryl and alkylaryl amide derivatives of phenothiazine have the ability to inhibit BuChE with no detectable inhibition of AChE. These selective BuChE inhibitors can be prepared with inhibitor potencies in the nanomolar concentration range. The ability of these aromatic phenothiazine derivatives to inhibit BuChE is often directly attributed to the total molecular volume of the inhibitor. However, certain steric, conformational, and electronic factors also influence inhibitor potency. The relatively nonpolar nature of the aryl and alkylaryl phenothiazine amides suggests that these molecules could readily cross the blood–brain barrier for the effective treatment of dementias such as Alzheimer's disease. The BuChE-specific characteristics of these aromatic phenothiazine amides could also provide an effective way to elucidate the role of BuChE in normal nervous system and in Alzheimer's disease.

### 4. Experimental

#### 4.1. Materials

Purified human plasma butyrylcholinesterase (BuChE, EC 3.1.1.8) was a gift from Dr. Oksana Lockridge (University of Nebraska Medical Center). Purified recombinant human acetylcholinesterase (AChE, EC 3.1.1.7), acetylthiocholine, butyrylthiocholine, 5,5'-dithiobis (2-nitrobenzoic acid) (DTNB), and phenothiazine were purchased from Sigma (St. Louis, MO). Acid chlorides were purchased from Aldrich Chemical Co. Inc. (Milwaukee, WI) and used without further purification. For those unavailable commercially, acid chlorides were prepared from the corresponding acids which were also purchased from Aldrich.

#### 4.2. Synthesis of compounds

A solution containing phenothiazine (5.1 mmol), acid chloride (10.5–30 mmol), and triethylamine (5.1 mmol) in dichloromethane (50 mL) was refluxed with stirring until TLC analysis revealed that all phenothiazine was consumed. Reaction periods ranged from 17 h to 20

days. The cooled reaction mixture was then washed successively with 5% aqueous sodium bicarbonate (3× 50 mL), 5% hydrochloric acid (3× 50 mL) followed by water (2× 50 mL). The solution was dried (MgSO<sub>4</sub>), filtered, and solvent evaporated under vacuum. The crude solid product was then routinely purified by column chromatography using silica gel 60 (63–200 $\mu$ ) (Caledon Laboratories Ltd) as adsorbant and dichloromethane or a dichloromethane/ethyl acetate mixture as eluent. Fractions containing only the desired product were combined, the solvent evaporated under vacuum. The product was crystallized from petroleum ether/dichloromethane (2:1). Yields of purified amides varied from 8% to 70% (average 46%). No attempt was made to optimize the yield.

Acid chlorides were synthesized from the corresponding carboxylic acid using oxalyl chloride, as described previously.<sup>25</sup>

### 4.3. Analysis of synthesized compounds

Melting points were determined on a Mel-Temp II apparatus and are uncorrected. Thin layer chromatography was carried out using silica gel sheets with fluorescent indicator (0.20 mm thickness; Macherey–Nagel) and dichloromethane or a dichloromethane/ethyl acetate mixture as developing solvent. Plates were visualized using a short wavelength UV lamp. Infrared spectra were recorded as Nujol mulls between sodium chloride plates on a Nicolet Model 205 or a Nicolet Avatar 330 FT-IR spectrometer. Peak positions were reproducible within 1–2 cm<sup>-1</sup>. Nuclear magnetic resonance spectra were recorded at the Atlantic Region Magnetic Resonance Centre, Dalhousie University, on a Bruker AC-250F operating at 250.1 MHz for proton and 62.9 MHz for carbon or a Bruker AVANCE 500 operating at 500.13 MHz for proton and 125.76 MHz for carbon-13. Chemical shifts are reported in ppm relative to TMS, in CDCl<sub>3</sub> or DMSO-d<sub>6</sub> solution. Mass spectra were recorded at Dalhousie University on a CEC 21-110B spectrometer using electron ionization at 70 V and an appropriate source temperature with samples being introduced by means of a heatable port probe. Accurate mass measurements were also made on this machine operated at a mass resolution of 8000 by computer controlled peak matching to appropriate PFK reference ions. Mass measurements were routinely within 3 ppm of the calculated value.

### 4.4. Analytical data

The melting point (mp), IR, <sup>1</sup>H NMR, <sup>13</sup>C NMR, and HR-MS data are listed below for each synthesized compound.

**4.4.1. Benzoyl phenothiazine (1).** Colorless needles, mp 174.5–176 °C (lit. mp 174 °C.<sup>32</sup>) IR (Nujol): 1673, 1322, 1259, 1110, 1029, 873, 855, 767, 752, 704, 689 cm<sup>-1</sup>. <sup>1</sup>H NMR (CDCl<sub>3</sub>): 7.09–7.47 (overlapping m). <sup>13</sup>C NMR (CDCl<sub>3</sub>): 126.53, 126.98, 127.20, 127.77, 128.07, 128.93, 130.46, 132.32, 135.28, 139.54, 168.97. EI-MS (*m/z*): 303 (M<sup>+</sup>), 198, 154, 127, 105 (base), 77,

69, 63, 51. HR-MS (EI): M<sup>+</sup> found, 303.0710; calcd for C<sub>19</sub>H<sub>13</sub>NOS, 303.0718.

**4.4.2. 2-Methylbenzoyl phenothiazine (2).** Off-white crystals, mp 159.5–160.9 °C. IR (Nujol): 1668, 1321, 1259, 1237, 1043, 960, 854, 760, 756, 727, 647, 623 cm<sup>-1</sup>. <sup>1</sup>H NMR (CDCl<sub>3</sub>): 2.46 (broad s, 3H), 6.9–7.5 (overlapping m, 12H). <sup>13</sup>C NMR (CDCl<sub>3</sub>): 19.40, 125.22, 126.49, 126.67, 127.02, 127.44, 127.56, 129.21, 130.26, 132.30, 135.36, 135.59, 138.47, 169.33. EI-MS (*m/z*): 317 (M<sup>+</sup>), 199, 198, 167, 166, 154, 120, 119 (base), 91, 65. HR-MS (EI): M<sup>+</sup> found, 317.0877; calcd for C<sub>20</sub>H<sub>15</sub>NOS, 317.0874.

**4.4.3. 3-Methylbenzoyl phenothiazine (3).** Colorless crystals, mp 140–142 °C. IR (Nujol): 1656, 1584, 1321, 1309, 1262, 1189, 805, 764, 756 cm<sup>-1</sup>. <sup>1</sup>H NMR (CDCl<sub>3</sub>): 2.26 (s, 3H), 7.0–7.5 (overlapping m, 12H). <sup>13</sup>C NMR (CDCl<sub>3</sub>): 21.28, 125.86, 126.39, 126.86, 127.12, 127.64, 129.60, 131.13, 132.25, 135.09, 137.86, 139.53, 169.03. EI-MS (*m/z*): 317 (M<sup>+</sup>), 199, 198, 154, 119 (base), 91. HR-MS (EI): M<sup>+</sup> found, 317.0874; calcd for C<sub>20</sub>H<sub>15</sub>NOS, 317.0874.

**4.4.4. 3-Bromobenzoyl phenothiazine (4).** Colorless crystals, mp 139.5–141.3 °C. IR (Nujol): 1667, 1566, 1324, 1262, 1157, 771, 754 cm<sup>-1</sup>. <sup>1</sup>H NMR (CDCl<sub>3</sub>): 7.03 (t, *J* = 7.9 Hz, 1H), 7.15–7.20 (overlapping m, 5H), 7.36–7.47 (overlapping m, 5H), 7.61 (t, *J* = 1.8 Hz, 1H). <sup>13</sup>C NMR (CDCl<sub>3</sub>): 122.15, 126.69, 127.00, 127.21, 127.74, 129.37, 132.01, 132.27, 133.38, 137.13, 139.05, 167.19. EI-MS (*m/z*): 383 (M<sup>+</sup>, <sup>81</sup>Br), 381 (M<sup>+</sup>, <sup>79</sup>Br) (base), 200, 199, 198, 197, 185, 183, 166, 157, 155, 154. HR-MS (EI): M<sup>+</sup>, <sup>79</sup>Br found, 380.9805; calcd for C<sub>19</sub>H<sub>12</sub>NOSBr, 380.9823.

**4.4.5. 4-Methylbenzoyl phenothiazine (5).** Colorless crystals, mp 197–199 °C. IR (Nujol): 1660, 1609, 1588, 1329, 1265, 1182, 828, 770, 753 cm<sup>-1</sup>. <sup>1</sup>H NMR (CDCl<sub>3</sub>): 2.29 (s, 3H), 7.01 (d, *J* = 8.3 Hz, 2H), 7.11–7.47 (overlapping m, 10H). <sup>13</sup>C NMR (CDCl<sub>3</sub>): 21.46, 126.33, 126.89, 127.10, 127.66, 128.63, 129.05, 132.20, 139.69, 140.74, 168.86. EI-MS (*m/z*): 317 (M<sup>+</sup>), 198, 154, 127, 119 (base), 91, 89, 69, 65, 63. HR-MS (EI): M<sup>+</sup> found, 317.0874; calcd for C<sub>20</sub>H<sub>15</sub>NOS, 317.0874.

**4.4.6. 4-Bromobenzoyl phenothiazine (6).** Colorless crystals, mp 166–168 °C (lit. mp 162–163 °C.<sup>33</sup>) IR (Nujol): 1666, 1587, 1329, 1263, 1109, 1072, 1011, 958, 838, 755 cm<sup>-1</sup>. <sup>1</sup>H NMR (CDCl<sub>3</sub>): 7.15–7.19 (overlapping m, 4H), 7.23 (d, *J* = 8.5 Hz, 2H), 7.34–7.45 (overlapping m, 6H). <sup>13</sup>C NMR (CDCl<sub>3</sub>): 124.92, 126.60, 126.96, 127.01, 127.72, 130.49, 131.22, 132.16, 134.04, 139.18, 167.75. EI-MS (*m/z*): 383 (M<sup>+</sup>, <sup>81</sup>Br), 381 (M<sup>+</sup>, <sup>79</sup>Br), 200, 199, 198 (base), 196, 186, 185, 184, 183, 166, 157, 155. HR-MS (EI): M<sup>+</sup> found, 380.9808; calcd for C<sub>19</sub>H<sub>12</sub>NOSBr, 380.9823.

**4.4.7. 4-Methoxybenzoyl phenothiazine (7).** Colorless crystals, mp 170–175 °C (lit. mp 173–174 °C.<sup>34</sup>) IR (Nujol): 1657, 1608, 1512, 1326, 1258, 1175, 1029, 840, 768, 760 cm<sup>-1</sup>. <sup>1</sup>H NMR (CDCl<sub>3</sub>): 3.75 (s, 3H), 6.70 (d, *J* = 8.6 Hz, 2H), 7.11–7.20 (overlapping m, 4H), 7.33

(d,  $J = 8.6$  Hz, 2H), 7.39–7.47 (overlapping m, 4H).  $^{13}\text{C}$  NMR ( $\text{CDCl}_3$ ): 55.25, 113.23, 126.26, 126.93, 127.06, 127.27, 127.66, 131.14, 132.13, 139.91, 161.26, 168.34. EI-MS ( $m/z$ ): 333 ( $\text{M}^+$ ), 198, 154, 136, 135 (base), 107, 92, 77, 64, 63. HR-MS (EI):  $\text{M}^+$  found, 333.0819; calcd for  $\text{C}_{20}\text{H}_{15}\text{NO}_2\text{S}$ , 333.0823.

**4.4.8. 4-Acetoxybenzoyl phenothiazine (8).** Colorless crystals, mp 185–187 °C. IR (Nujol): 1762, 1650, 1601, 1333, 1267, 1205, 1169, 913, 855, 757  $\text{cm}^{-1}$ .  $^1\text{H}$  NMR ( $\text{CDCl}_3$ ): 2.24 (s, 3H), 6.96 (d,  $J = 8.8$  Hz, 2H), 7.13–7.19 (overlapping m, 4H), 7.37–7.48 (overlapping m, 6H).  $^{13}\text{C}$  NMR ( $\text{CDCl}_3$ ): 21.05, 121.07, 126.47, 126.92, 127.01, 127.64, 130.33, 132.13, 132.49, 139.33, 152.03, 167.80, 168.65. EI-MS ( $m/z$ ): 361 ( $\text{M}^+$ , base), 199, 198, 167, 163, 154, 121. HR-MS (EI):  $\text{M}^+$  found, 361.0767; calcd for  $\text{C}_{20}\text{H}_{15}\text{NO}_3\text{S}$ , 361.0772.

**4.4.9. 4-Nitrobenzoyl phenothiazine (9).** Yellow crystals, mp 225–227 °C (lit. mp 225–226 °C.<sup>34</sup>) IR (Nujol): 1662, 1601, 1519, 1506, 1343, 1264, 1106, 861, 765, 750  $\text{cm}^{-1}$ .  $^1\text{H}$  NMR ( $\text{CDCl}_3$ ): 7.15–7.57 (overlapping m, 10H), 8.07 (d,  $J = 8.9$  Hz, 2H).  $^{13}\text{C}$  NMR ( $\text{CDCl}_3$ ): 123.51, 127.12, 127.26, 127.36, 128.12, 129.91, 132.51, 138.86, 141.55, 148.78, 166.99. EI-MS ( $m/z$ ): 348 ( $\text{M}^+$ ), 199, 198 (base), 154, 127, 120, 104, 92, 76, 50. HR-MS (EI):  $\text{M}^+$  found, 348.0573; calcd for  $\text{C}_{19}\text{H}_{12}\text{N}_2\text{O}_3\text{S}$ , 348.0568.

**4.4.10. 4-*tert*-Butylbenzoyl phenothiazine (10).** Colorless crystals, mp 177.5–179 °C (lit. mp 171–173 °C.<sup>35</sup>) IR (Nujol): 1667, 1330, 1261, 1118, 832, 764, 748  $\text{cm}^{-1}$ .  $^1\text{H}$  NMR ( $\text{CDCl}_3$ ): 1.24 (s, 9H), 7.11–7.44 (overlapping m, 12H).  $^{13}\text{C}$  NMR ( $\text{CDCl}_3$ ): 31.20, 34.89, 124.95, 126.42, 126.94, 127.22, 127.72, 128.96, 132.20, 132.28, 139.76, 153.92, 168.89. EI-MS ( $m/z$ ): 359 ( $\text{M}^+$ ), 198, 161 (base), 146, 118, 117, 91, 77. HR-MS (EI):  $\text{M}^+$  found, 359.1341; calcd for  $\text{C}_{23}\text{H}_{21}\text{NOS}$ , 359.1344.

**4.4.11. 4-Biphenylcarbonyl phenothiazine (11).** Colorless crystals, mp 220.5–222 °C. IR (Nujol): 1660, 1336, 1263, 842, 763, 753, 694  $\text{cm}^{-1}$ .  $^1\text{H}$  NMR ( $\text{CDCl}_3$ ): 7.15–7.57 (overlapping m).  $^{13}\text{C}$  NMR ( $\text{CDCl}_3$ ): 126.50, 126.61, 127.00, 127.13 (2 peaks), 127.74, 127.92, 128.88, 129.57, 132.23, 133.92, 139.55, 139.96, 143.08, 168.61. EI-MS ( $m/z$ ): 379 ( $\text{M}^+$ ) (base), 199, 198, 182, 181, 153, 152. HR-MS (EI):  $\text{M}^+$  found, 379.1025; calcd for  $\text{C}_{25}\text{H}_{17}\text{NOS}$ , 379.1031.

**4.4.12. Phenylacetyl phenothiazine (12).** Colorless needles, mp 152.5–154 °C (lit. mp 152–153 °C.<sup>36</sup>) IR (Nujol): 1681, 1661, 1341, 1255, 1166, 1124, 1029, 771, 759, 703  $\text{cm}^{-1}$ .  $^1\text{H}$  NMR ( $\text{CDCl}_3$ ): 3.81 (s, 2H), 7.04–7.24 (overlapping m, 7H), 7.26–7.34 (m, 2H), 7.37 (dd,  $J = 7.6$  and 1.5 Hz, 2H), 7.52 (broad d,  $J = 7.6$  Hz, 2H).  $^{13}\text{C}$  NMR ( $\text{CDCl}_3$ ): 41.23, 126.88, 127.01 (2 peaks), 127.38, 127.97, 128.47, 129.03, 133.57, 134.52, 138.76, 170.31. EI-MS ( $m/z$ ): 317 ( $\text{M}^+$ ), 200, 199, 198 (base), 171, 167, 166, 154, 127, 91, 69, 65, 63. HR-MS (EI):  $\text{M}^+$  found, 317.0874; calcd for  $\text{C}_{20}\text{H}_{15}\text{NOS}$ , 317.0874.

**4.4.13. 2-Phenylpropanoyl phenothiazine (13).** Pale yellow crystals, mp 112–114 °C. IR (Nujol): 1672, 1250,

1170, 1128, 1067, 1028, 965, 767, 755, 699  $\text{cm}^{-1}$ .  $^1\text{H}$  NMR ( $\text{CDCl}_3$ ): 1.46 (d,  $J = 7.0$  Hz, 3H), 4.13 (broad q,  $J = \sim 7$  Hz, 1H), 7.03–7.54 (overlapping m, 13H).  $^{13}\text{C}$  NMR ( $\text{CDCl}_3$ ): 20.57, 43.20, 126.75, 126.86, 127.37, 127.45, 127.63, 127.85, 127.96, 128.51, 138.71, 140.91, 173.48. EI-MS ( $m/z$ ): 331 ( $\text{M}^+$ ), 200, 199, 198 (base), 166, 154, 127, 105, 103, 79, 77. HR-MS (EI):  $\text{M}^+$  found, 331.1024; calcd for  $\text{C}_{21}\text{H}_{17}\text{NOS}$ , 331.1031.

**4.4.14. 3-Phenylpropanol phenothiazine (14).** Off-white crystals, mp 102–104 °C. IR (Nujol): 1673, 1577, 1310, 1249, 1124, 767, 753, 693.  $^1\text{H}$  NMR ( $\text{CDCl}_3$ ): 2.72–2.79 (m, 2H), 2.91–2.98 (m, 2H), 7.07–7.46 (overlapping m, 13H).  $^{13}\text{C}$  NMR ( $\text{CDCl}_3$ ): 31.46, 36.22, 126.20, 126.87, 127.04, 127.34, 128.04, 128.41, 128.50, 133.36, 138.76, 140.85, 171.38. EI-MS ( $m/z$ ): 331 ( $\text{M}^+$ ), 279, 199 (base), 167, 154, 133, 105, 91, 77. HR-MS (EI):  $\text{M}^+$  found, 331.1044; calcd for  $\text{C}_{21}\text{H}_{17}\text{NOS}$ , 331.1031.

**4.4.15. 2-Phenylbutanoyl phenothiazine (15).** Colorless crystals, mp 78–80 °C. IR (Nujol): 3027, 1679, 1279, 1252, 1243, 1167, 1128, 1031, 765, 752, 708, 699  $\text{cm}^{-1}$ .  $^1\text{H}$  NMR ( $\text{CDCl}_3$ ): 0.83 (broad t,  $J = \sim 7.2$  Hz, 3H), 1.70 (broad m,  $J = \sim 7$  Hz, 1H), 2.12 (broad m,  $J = \sim 7$  Hz, 1H), 3.82 (broad m, 1H), 7.1–7.6 (overlapping m, 13H).  $^{13}\text{C}$  NMR ( $\text{CDCl}_3$ ): 12.35, 28.67, 50.67, 126.96, 127.02, 127.10, 127.86, 128.09, 128.18 (2 peaks), 128.65, 139.22, 139.89, 172.91. EI-MS ( $m/z$ ): 345 ( $\text{M}^+$ ), 200, 199, 198, 119, 91 (base), 50, 40. HR-MS (EI):  $\text{M}^+$  found, 345.1186; calcd for  $\text{C}_{22}\text{H}_{19}\text{NOS}$ , 345.1187.

**4.4.16. 3-Phenylbutanoyl phenothiazine (16).** Colorless crystals, mp 117.5–120 °C. IR (Nujol): 1669, 1586, 1567, 1343, 1322, 1263, 1177, 1097, 767, 753  $\text{cm}^{-1}$ .  $^1\text{H}$  NMR ( $\text{CDCl}_3$ ): 1.22 (d,  $J = 7.0$  Hz, 3H), 2.62 (dd,  $J = 15.1$  and 8.4 Hz, 1H), 2.85 (dd,  $J = 15.1$  and 6.3 Hz, 1H), 3.28 (m, 1H), 7.0–7.6 (overlapping m, 13H).  $^{13}\text{C}$  NMR ( $\text{CDCl}_3$ ): 21.64, 36.83, 42.99, 126.59, 127.09 (2 peaks), 127.26, 127.67, 128.30, 128.76, 133.81, 139.09, 146.29, 171.09. EI-MS ( $m/z$ ): 345 ( $\text{M}^+$ ), 200, 199 (base), 198, 167, 166, 154, 105, 91, 79, 77. HR-MS (EI):  $\text{M}^+$  found, 345.1188; calcd for  $\text{C}_{22}\text{H}_{19}\text{NOS}$ , 345.1187.

**4.4.17. 4-Phenylbutanoyl phenothiazine (17).** Colorless crystals, mp 96.5–99 °C. IR (Nujol): 1668, 1580, 1259, 1126, 1031, 769, 754  $\text{cm}^{-1}$ .  $^1\text{H}$  NMR ( $\text{CDCl}_3$ ): 1.91 (tt,  $J = \sim 7.3$  Hz, 2H), 2.46 (t,  $J = 7.3$  Hz, 2H), 2.56 (t,  $J = 7.6$  Hz, 2H), 7.0–7.5 (overlapping m, 13H).  $^{13}\text{C}$  NMR ( $\text{CDCl}_3$ ): 26.87, 33.52, 34.96, 125.85, 126.81, 127.00, 127.31, 128.00, 128.32, 128.50, 133.33, 138.85, 141.60, 171.92. EI-MS ( $m/z$ ): 345 ( $\text{M}^+$ ), 200, 199 (base), 198, 167, 147, 91. HR-MS (EI):  $\text{M}^+$  found 345.1194; calcd for  $\text{C}_{22}\text{H}_{19}\text{NOS}$ , 345.1187.

**4.4.18. 4-Biphenylcarbonyl phenothiazine (18).** Colorless crystals, mp 150.5–153 °C. IR (Nujol): 1689, 1586, 1561, 1251, 1162, 1124, 764, 752, 738  $\text{cm}^{-1}$ .  $^1\text{H}$  NMR ( $\text{CDCl}_3$ ): 3.84 (s, 2H), 7.13–7.56 (overlapping m, 17H).  $^{13}\text{C}$  NMR ( $\text{CDCl}_3$ ): 41.08, 127.23, 127.31 (2 peaks), 127.40 (2 peaks), 127.47, 127.59, 128.19, 129.02, 129.69, 133.83, 138.97, 139.98, 141.13, 170.47. EI-MS ( $m/z$ ): 393 ( $\text{M}^+$ ), 200, 199 (base), 198, 168, 167, 166,

165, 154, 152, 91. HR-MS (EI):  $M^+$  found, 393.1173; calcd for  $C_{26}H_{19}NOS$ , 393.1187.

**4.4.19. 1-Naphthoyl phenothiazine (19).** Colorless crystals, mp 176–179 °C (lit. mp 170 °C.<sup>37</sup>) IR (Nujol): 1659, 1505, 1330, 1291, 1259, 1145, 1127, 810, 796, 769, 759  $cm^{-1}$ .  $^1H$  NMR ( $CDCl_3$ ): 7.0–7.9 (overlapping m, 14H), 8.36 (broad d,  $J = \sim 7.9$  Hz, 1H).  $^{13}C$  NMR ( $CDCl_3$ ): 124.49, 125.15, 125.90, 126.31, 126.61, 126.778, 127.12, 127.69, 128.37, 129.84, 132.29, 133.31, 138.85, 168.87. EI-MS ( $m/z$ ): 353 ( $M^+$ ), 200, 199, 198, 197, 196, 171, 166, 156, 155 (base), 154, 140, 127, 104. HR-MS (EI):  $M^+$  found, 353.0875; calcd for  $C_{23}H_{15}NOS$ , 353.0874.

**4.4.20. 2-Naphthoyl phenothiazine (20).** Colorless crystals, mp 190–192 °C (lit. mp 185 °C.<sup>37</sup>) IR (Nujol): 1659, 1628, 1322, 1260, 1192, 861, 822, 802, 755  $cm^{-1}$ .  $^1H$  NMR ( $CDCl_3$ ): 7.10–7.19 (overlapping m, 4H), 7.36 (dd,  $J = 8.6$  and 1.8 Hz, 1H), 7.46–7.54 (overlapping m, 6H), 7.64 (d,  $J = 8.6$  Hz, 1H), 7.75–7.81 (overlapping m, 2H), 8.08 (broad s, 1H).  $^{13}C$  NMR ( $CDCl_3$ ): 125.54, 126.69, 126.74, 127.21, 127.36, 127.69, 127.73, 127.90, 129.00, 130.10, 132.47, 132.74, 132.84, 134.22, 139.80, 169.00. EI-MS ( $m/z$ ): 353 ( $M^+$ ), 199, 198, 171, 166, 155 (base), 127, 101, 77. HR-MS (EI):  $M^+$  found, 353.0879; calcd for  $C_{23}H_{15}NOS$ , 353.0874.

**4.4.21. 1-Naphthylacetyl phenothiazine (21).** Off-white crystals, mp 137–139 °C. IR (Nujol): 1673, 1598, 1511, 1333, 1252, 1153, 1123, 793, 772, 760  $cm^{-1}$ .  $^1H$  NMR ( $CDCl_3$ ): 4.29 (s, 2H), 7.21–7.85 (overlapping m, 15H).  $^{13}C$  NMR ( $CDCl_3$ ): 39.13, 123.96, 125.58, 126.46, 127.20, 127.35, 127.46, 127.76, 127.86, 127.99, 128.25, 128.85, 131.51, 132.21, 133.61, 134.01, 139.04, 170.41. EI-MS ( $m/z$ ): 367 ( $M^+$ ), 200, 199, 198, 166, 154, 142 (base), 139, 127, 115. HR-MS (EI):  $M^+$  found, 367.1038; calcd for  $C_{24}H_{17}NOS$ , 367.1031.

**4.4.22. 2-Naphthylacetyl phenothiazine (22).** Pale yellow crystals, mp 181.5–183.5 °C. IR (Nujol): 1677, 1579, 1348, 1258, 1165, 1126, 980, 945, 865, 796, 767, 739  $cm^{-1}$ .  $^1H$  NMR ( $CDCl_3$ ): 4.02 (s, 2H), 7.21–7.82 (overlapping m, 15H).  $^{13}C$  NMR ( $CDCl_3$ ): 41.61, 125.85, 126.18, 127.18 (2 peaks), 127.41, 127.57, 127.82, 127.91, 128.13, 128.25, 132.19, 132.62, 133.66, 133.81, 139.01, 170.38. EI-MS ( $m/z$ ): 367 ( $M^+$ ), 201, 200, 199 (base), 198, 167, 166, 142, 141, 115. HR-MS (EI):  $M^+$  found, 367.1036; calcd for  $C_{24}H_{17}NOS$ , 367.1031.

**4.4.23. 9-Anthrylcarbonyl phenothiazine (23).** Bright yellow crystals, mp 212–213.5 °C. IR (Nujol): 1660, 1357, 1309, 1256, 1189, 1130, 950, 884, 844, 762, 650  $cm^{-1}$ .  $^1H$  NMR ( $CDCl_3$ ): 6.33 (dt,  $J = 7.7$  and 1.3 Hz, 1H), 6.44 (dd,  $J = 8.2$  and 1.1 Hz, 1H), 6.71 (dt,  $J = 7.5$  and 1.3 Hz, 1H), 7.14 (dd,  $J = 7.5$  and 1.3 Hz, 1H), 7.28–7.38 (overlapping m, 3H), 7.53 (dt,  $J = 7.7$  and 1.3 Hz, 1H), 7.58 (m, 2H), 7.76 (broad t,  $J = \sim 7.2$  Hz, 1H), 7.82 (broad d,  $J = \sim 7.5$  Hz, 1H), 8.07 (d,  $J = 8.8$  Hz, 1H), 8.16 (dd,  $J = 7.9$  and 1.3 Hz, 1H), 8.20 (broad d,  $J = 8.4$  Hz, 1H), 8.39 (s, 1H), 8.55 (d,  $J = 8.8$  Hz, 1H).  $^{13}C$  NMR ( $CDCl_3$ ): 125.10, 125.38 (2 peaks), 125.65,

125.68, 126.27, 126.57, 126.70, 127.24, 127.34, 127.45, 127.67, 127.74, 128.09, 128.33 (2 peaks), 128.59, 129.29, 130.18, 130.24, 130.74, 131.08, 132.57, 132.79, 138.10, 138.25, 169.16. EI-MS ( $m/z$ ): 403 ( $M^+$ ), 206, 205 (base), 199, 198, 178, 177, 176, 152, 92. HR-MS (EI):  $M^+$  found, 403.1033; calcd for  $C_{27}H_{17}NOS$ , 403.1031.

**4.4.24. trans-3-Phenylpropenoyl phenothiazine (24).** Pale yellow crystals, mp 137–138.5 °C (lit. mp 139–140 °C.<sup>38</sup>) IR (Nujol): 3063, 1668, 1618, 1576, 1336, 1250, 1168, 979, 765, 755  $cm^{-1}$ .  $^1H$  NMR ( $CDCl_3$ ): 6.74 (d,  $J = 15.4$  Hz, 1H), 7.21–7.50 (overlapping m, 11H), 7.64 (d,  $J = 7.6$  Hz, 2H), 7.86 (d,  $J = 15.4$  Hz, 1H).  $^{13}C$  NMR ( $CDCl_3$ ): 118.43, 126.82, 126.93, 127.26, 127.94, 128.10, 128.85, 130.01, 132.75, 134.97, 138.61, 143.78, 164.42. EI-MS ( $m/z$ ): 329 ( $M^+$ ), 200, 199 (base), 198, 167, 131, 103, 77. HR-MS (EI):  $M^+$  found, 329.0874; calcd for  $C_{21}H_{15}NOS$ , 329.0874.

**4.4.25. Oxalyl(di)phenothiazine (25).** Off-white crystals, mp 300.5–303.5 °C. IR (Nujol): 1681, 1661, 1583, 1309, 1284, 1262, 1236, 1186, 757  $cm^{-1}$ .  $^1H$  NMR ( $DMSO-d_6$ ): 7.2–7.7 (overlapping m).  $^{13}C$  NMR ( $CDCl_3$ ): 125.62, 126.86, 126.95, 127.25, 127.39, 127.53, 128.09, 128.26, 131.10, 133.53, 135.10, 135.44, 163.35. EI-MS ( $m/z$ ): 452 ( $M^+$ ), 424, 200, 199, 198, 167, 166, 154, 86, 51, 49 (base). HR-MS (EI):  $M^+$  found, 452.0654; calcd for  $C_{26}H_{16}N_2O_2S_2$ , 452.0653.

#### 4.5. Enzyme kinetic studies

The esterase activity of AChE and BuChE was determined by a modification of the Ellman method.<sup>28</sup> Briefly, 2.7 mL of buffered DTNB solution (pH 8.0), 0.1 mL of human recombinant AChE (0.03  $U^{13}$ ) or purified human serum BuChE (0.05  $U^{13}$ ) in 0.005% aqueous gelatin, and 0.1 mL of 50% aqueous acetonitrile or one of the phenothiazine derivatives, dissolved in this solvent, were placed in a quartz cuvette of 1 cm path-length. Serial (1:10) dilutions of each compound in 50% acetonitrile were tested for the ability to inhibit either AChE or BuChE. The mixture was zeroed at 412 nm, and the reaction initiated by the addition of acetylthiocholine or butyrylthiocholine in aqueous solution at a final concentration of  $1.6 \times 10^{-4}$  M. The reactions were performed at 23 °C. The rate of change of absorbance ( $\Delta A/min$ ), reflecting the rate of hydrolysis of acetylthiocholine or butyrylthiocholine, was recorded every 5 s for 1 min, using a Milton-Roy 1201 UV-visible spectrophotometer (Milton-Roy, Ivyland, PA) set at  $\lambda = 412$  nm. These experiments were generally done at least in triplicate and the values averaged. Lineweaver–Burk plots were generated by using a fixed amount of cholinesterase and varying amounts of substrate ( $3 \times 10^{-5}$  M– $1.6 \times 10^{-4}$  M) in the presence or absence of the inhibitors. The re-plot of the slopes of the above double reciprocal plots against inhibitor concentration gave the inhibitor constant ( $K_i$ ) as the intercept on the  $x$ -axis.

#### 4.6. Calculation of log $P$ values

In order to assess the ability of the compound to cross the hydrophobic blood–brain barrier, log  $P$  values were

obtained using the ALOGPS method.<sup>30</sup> The ALOGPS methodology employs a large collection of compounds taken from the PHYSPROP database of Syracuse Research Corporation (Syracuse Research Corporation, Physical/Chemical Property Database (PHYSPROP); SRC Environmental Science Center: Syracuse, NY, 1994). This methodology is a statistical approach, involving electrotopological state (E-state) indices and neural network ensembles.

#### 4.7. Calculation of molecular parameters

Molecular mechanics calculations were carried out using the MMFF94 force field (PC Spartan Pro, Wavefunction, Inc., 18401 Von Karman, Suite 370, Irvine, California, 92612). Geometry optimizations were carried out at this level of theory, based on the best conformer. This optimized structure was employed in a subsequent Hartree–Fock/STO-3G calculation. Hartree–Fock calculations were carried out using the Gaussian 98 suite of programs.<sup>29</sup> The molecular volume was obtained at this level of theory by selecting a surface of fixed electron density (0.001 e/bohr<sup>3</sup>, in this case), and by computing the volume within that isodensity surface.<sup>39</sup> The volume = tight option was employed in order to obtain increased accuracy. Molecular volumes reported in the paper are based on an average of five separate volume calculations. The structure for the graphical abstract as well as Figure 3 were generated using the HyperChem<sup>®</sup> program.<sup>42</sup>

#### Acknowledgments

Canadian Institutes of Health Research, Vascular Health and Dementia Initiative (DOV-78344) (through partnership of Canadian Institutes of Health Research, Heart & Stroke Foundation of Canada, the Alzheimer Society of Canada, and Pfizer Canada Inc.), Natural Sciences and Engineering Research Council of Canada, Capital District Health Authority Research Fund, Nova Scotia Health Research Foundation, Brain Tumour Foundation of Canada, and the Committee on Research and Publications of Mount Saint Vincent University are acknowledged. We thank Andrew Reid and Andrea LeBlanc for their technical help.

#### References and notes

- Perry, E. K.; Perry, R. H.; Blessed, G.; Tomlinson, E. *Neuropath. Appl. Neurobiol.* **1978**, *4*, 273.
- Whitehouse, P. J.; Price, D. L.; Clark, A. W.; Coyle, J. T.; DeLong, M. R. *Ann. Neurol.* **1981**, *10*, 122.
- Bartus, R. T.; Dean, R. L. I.; Beer, B.; Lippa, A. S. *Science* **1982**, *217*, 408.
- Coyle, J. T.; Price, D. L.; DeLong, M. R. *Science* **1983**, *219*, 1184.
- Silver, A. *The Biology of Cholinesterases*; Elsevier: Elsevier, 1974.
- Birks, J. *Cochrane Database Syst. Rev.* **2006**, *1*, CD005593.
- Perry, E. K.; Tomlinson, B. E.; Blessed, G.; Bergmann, K.; Gibson, P. H.; Perry, R. H. *Br. Med. J.* **1978**, *2*, 1457.

- Atack, J. R.; Perry, E. K.; Bonham, J. R.; Candy, J. M.; Perry, R. H. *J. Neurochem.* **1987**, *48*, 1687.
- Arendt, T.; Bruckner, M. K.; Lange, M.; Bigl, V. *Neurochem. Int.* **1992**, *21*, 381.
- Darvesh, S.; Hopkins, D. A.; Geula, C. *Nat. Rev. Neurosci.* **2003**, *4*, 131.
- Darvesh, S.; MacKnight, C.; Rockwood, K. *Int. Psychogeriatr.* **2001**, *13*, 461.
- Greig, N. H.; Utsuki, T.; Ingram, D. K.; Wang, Y.; Pepeu, G.; Scali, C.; Yu, Q. S.; Mamczarz, J.; Holloway, H. W.; Giordano, T.; Chen, D.; Furukawa, K.; Sambamurti, K.; Brossi, A.; Lahiri, D. K. *Proc. Natl. Acad. Sci. U.S.A.* **2005**, *102*, 17213.
- Darvesh, S.; Walsh, R.; Kumar, R.; Caines, A.; Roberts, S.; Magee, D.; Rockwood, K.; Martin, E. *Alzheimer Dis. Assoc. Disord.* **2003**, *17*, 117.
- Greig, N. H.; Lahiri, D. K.; Sambamurti, K. *Int. Psychogeriatr.* **2002**, *14*, 77.
- Sugimoto, H. *Chem. Rec.* **2001**, *1*, 63.
- Marco-Contelles, J.; do Carmo Carreiras, M.; Rodriguez, C.; Villarroya, M.; Garcia, A. G. *Chem. Rev.* **2006**, *106*, 116.
- Giacobini, E. In *Cholinesterases and Cholinesterase Inhibitors*; Giacobini, E., Ed.; Martin Dunitz: London and New York, 2000; pp 181–226.
- Weinstock, M.; Razin, M.; Chorev, M.; Enz, A. *J. Neural Transm. Suppl.* **1994**, *43*, 219.
- Sussman, J. L.; Harel, M.; Frolow, F.; Oefner, C.; Goldman, A.; Toker, L.; Silman, I. *Science* **1991**, *253*, 872.
- Nicolet, Y.; Lockridge, O.; Masson, P.; Fontecilla-Camps, J. C.; Nachon, F. *J. Biol. Chem.* **2003**, *278*, 41141, PDB ID: 1POL.
- Kryger, G.; Silman, I.; Sussman, J. L. *J. Physiol. Paris* **1998**, *92*, 191.
- Saxena, A.; Fedorko, J. M.; Vinayaka, C. R.; Medhekar, R.; Radić, Z.; Taylor, P.; Lockridge, O.; Doctor, B. P. *Eur. J. Biochem.* **2003**, *270*, 4447.
- Darvesh, S.; McDonald, R. S.; Darvesh, K. V.; Mataija, D.; Mothana, S.; Cook, H.; Carneiro, K. M.; Richard, N.; Walsh, R.; Martin, E. *Bioorg. Med. Chem.* **2006**, *14*, 4586.
- Saxena, A.; Redman, A. M.; Jiang, X.; Lockridge, O.; Doctor, B. P. *Biochemistry* **1997**, *36*, 14642.
- Darvesh, S.; McDonald, R. S.; Penwell, A.; Conrad, S.; Darvesh, K. V.; Mataija, D.; Gomez, G.; Caines, A.; Walsh, R.; Martin, E. *Bioorg. Med. Chem.* **2005**, *13*, 211.
- Radić, Z.; Pickering, N. A.; Vellom, D. C.; Camp, S.; Taylor, P. *Biochemistry* **1993**, *32*, 12074.
- Debord, J.; Merle, L.; Bollinger, J. C.; Dantoine, T. J. *Enzyme Inhib. Med. Chem.* **2002**, *17*, 197.
- Ellman, G. L.; Courtney, K. D.; Andres, V. J.; Featherstone, R. M. *Biochem. Pharmacol.* **1961**, *7*, 88.
- Frisch, M. J.; Trucks, G. W.; Schlegel, H. B.; Scuseria, G. E.; Robb, M. A.; Cheeseman, J. R.; Zakrzewski, V. G.; Montgomery, Jr., J. A.; Stratmann, R. E.; Burant, J. C.; Dapprich, S.; Millam, J. M.; Daniels, A. D.; Kudin, K. N.; Strain, M. C.; Farkas, O.; Tomasi, J.; Barone, V.; Cossi, M.; Cammi, R.; Mennucci, B.; Pomelli, C.; Adamo, C.; Clifford, S.; Ochterski, J.; Petersson, G. A.; Ayala, P. Y.; Cui, Q.; Morokuma, K.; Rega, N.; Salvador, P.; Dannenberg, J. J.; Malick, D. K.; Rabuck, A. D.; Raghavachari, K.; Foresman, J. B.; Cioslowski, J.; Ortiz, J. V.; Baboul, A. G.; Stefanov, B. B.; Liu, G.; Liashenko, A.; Piskorz, P.; Komaromi, I.; Gomperts, R.; Martin, R. L.; Fox, D. J.; Keith, T.; Al-Laham, M. A.; Peng, C. Y.; Nanayakkara, A.; Challacombe, M.; Gill, P. M. W.; Johnson, B.; Chen, W.; Wong, M. W.; Andres, J. L.; Gonzalez, C.; Head-Gordon, M.; Replogle, E. S.; Pople, J. A. Gaussian 98, Revision A.11.2. Gaussian, Inc., Pittsburgh PA, 2001.

30. Tetko, I. V.; Tanchuk, V. Y.; Villa, A. E. *J. Chem. Inf. Comput. Sci.* **2001**, *41*, 1407.
31. Baldessarini, R. J.; Tarazi, F. I. In *Goodman and Gilman's the Pharmacological Basis of Therapeutics*; Hardman, J. G., Limbird, L. E., Gilman, A. G., Eds., Tenth Ed.; McGraw-Hill Companies Inc.: New York, 2001; pp 485–520.
32. Cauquil, G.; Casadevall, A. *Compt. Rend.* **1953**, *236*, 1569.
33. Podolesov, B. D.; Kamceva, L. G. Godisen Zbornik-Prirodno-Matematicki Fakultet na Univerzitetot Kiril i Metodij-Skopje, Sekcija A: Matematika, Fizika i Hemija, **1969**, *19*, 91.
34. Mackie, A.; Cutler, A. A. *J. Chem. Soc.* **1954**, 2577.
35. Fischer, H.; Buerger, W. Swiss Patent No. CH 653675 AD, 1986.
36. Gilman, H.; Nelson, R. D. *J. Am. Chem. Soc.* **1953**, *75*, 5422.
37. Podolesov, B. D.; Kamceva, L. G. Godisen Zboinik-Prirodno-Matematicki Fakultet na Univerzitetot Kiril i Metodij-Skopje, Sekcija A: Matematika, Fizika i Hemija, **1971**, *21*, 39.
38. El-Maghraby, M. A.; Hassan, Kh. M. *J. Indian Chem. Soc.* **1976**, *53*, 1030.
39. Frisch, A.; Frisch, M. J. *Gaussian 98 User's Reference*, 2nd ed. Gaussian Inc., Pittsburg, PA, 1999.
40. Berman, H. M.; Westbrook, J.; Feng, Z.; Gilliland, G.; Bhat, T. N.; Weissig, H.; Shindyalov, I. N.; Bourne, P. E. The Protein Data Bank. *Nucleic Acids Res.*, **2000**, *28*, 235. <http://www.pdb.org/>.
41. DeLano, W. L. The PyMOL Molecular Graphics System. DeLano Scientific, San Carlos, CA, USA, 2002. <http://www.pymol.org>.
42. HyperChem<sup>®</sup> Release 7.51 for Windows<sup>®</sup>, copyright ©2002, Hypercube, Inc.